Properties of Barrier Components in a Composite Cover after 14 Years of Service and Differential Settlement

Joseph Scalia IV, A.M.ASCE[1]; Craig H. Benson, F.ASCE[2]; William H. Albright[3]; Benjamin S. Smith, M.ASCE[4]; and Xiaodong Wang[5]

Abstract: A case study is presented describing the effects of age (14 years) and differential settlement (≈0.3 m vertical over ≈0.4 m horizontal along a horizontal distance of ≈10 m) on the engineering properties of a soil barrier layer, a geosynthetic clay liner (GCL), and a geomembrane within a composite cover. Samples of the soil barrier layer had hydraulic conductivity below the design requirement of 5.0×10^{-7} m/s, except in areas that were cracked because of differential settlement. Tests showed that the geomembrane exceeded design specifications for tensile yield strength (≥22.9 kN/m) and elongation at tensile yield (≥13.0%), and current standard specifications for oxidative induction time (≥100 min) and stress crack resistance (≥500 h). Geomembrane seams also exceeded design specifications for peel strength (≥15.9 kN/m) and shear strength (≥22.9 kN/m). Geosynthetic clay liner samples showed a reduction in swell index relative to the as-built condition (from 27.9 to 21.0–24.5 mL/2 g) because of cation exchange. However, all GCL samples had hydraulic conductivity below the design requirement of 4×10^{-11} m/s. **DOI: 10.1061/(ASCE)GT.1943-5606.0001744.** © *2017 American Society of Civil Engineers.*

Author keywords: Geosynthetics; Geosynthetic clay liner; Landfill final cover; Composite cover; Field condition; Differential settlement.

Introduction

Conventional final covers employ barrier layers with low-hydraulic conductivity to control percolation into underlying waste. Long-term stability of these barrier components is critical to the overall performance of the containment facility. This is particularly important in low-level radioactive waste (LLW) disposal facilities, which are required to have a service life in excess of 1,000 years. Field studies evaluating the in-service properties of composite barrier materials in final covers are limited, despite recommendations from the National Academies for collection of these types of data (Mitchell et al. 2007), and none have been conducted for composite barriers that have settled differentially or at LLW disposal facilities (Benson et al. 2010, 2011). Independent technical reviews of waste management operations at existing and proposed LLW disposal facilities operated by the U.S. Department of Energy (DOE) identify long-term performance of final covers, and the impact of waste subsidence on the long-term effectiveness of final covers, as an unresolved technological issues (Adams et al. 2009).

Exhumation and sampling of final-cover components was conducted in 2012 at the Barnwell Disposal Facility in South Carolina (henceforth, the Site), which is used for LLW disposal. Samples were collected as part of repair activates from a location affected by differential settlement, and at unaffected adjacent locations. Differential settlement is defined in this paper for final covers as localized vertical distortions of the cover system components; these distortions may cause unacceptable tensile stresses or strains or the change of slopes, which may affect cover system performance. When an unacceptable magnitude of differential settlement is not provisioned during cover design, engineering judgment is required to identify when differential settlement merits repair. Differential settlement at the Site of approximately 0.3 m (vertical) over approximately 0.4 m (horizontal) along a horizontal distance of approximately 10 m was determined to warrant investigation and repair.

Landfilling of LLW was conducted at the Site in a series of unlined trenches approximately 15–90-m wide by 6–9-m deep, and 180–300-m long (SCDHEC 2007). Final cover is placed over the trenches for long-term containment. The Site has a conventional composite cover consisting of (from bottom): (1) a soil barrier layer composed of a clayey sand as described in Table 1 (design specifications and as-built properties), (2) a ≈ 10-mm thick geosynthetic clay liner (GCL) sold commercially as Bentofix NS (Albarrie Naue Ltd., Ottawa, California) as described in Table 2, (3) a 1.5-mm thick high-density polyethylene (HDPE) geomembrane as described in Table 3 (design specifications and as-built properties), (4) a 300-mm sand drainage layer, and (5) a 600-mm vegetated topsoil layer (the combined 900-mm soil layer overlying the geomembrane is predicted to prevent freezing of the underlying barrier layers). Repair activities conducted by site personnel involved removal of cover materials to the subgrade, repair of the soil barrier, installation of new geosynthetics, and replacement of the overlying earthen cover materials to design specifications.

Samples of the soil barrier, GCL, and geomembrane layers were collected by the authors for laboratory analysis of physical and chemical properties when the cover was repaired. Exhumed samples of the soil barrier and GCL were tested for saturated hydraulic

[1]Assistant Professor, Dept. of Civil and Environmental Engineering, Colorado State Univ., Fort Collins, CO 80523 (corresponding author). E-mail: joseph.scalia@colostate.edu

[2]Dean, School of Engineering and Applied Science, Univ. of Virginia, Charlottesville, VA 22904. E-mail: chbenson@virgina.edu

[3]Research Hydrogeologist Emeritus, Desert Research Institute, Reno, NV 89512. E-mail: bill.albright@dri.edu

[4]Project Manager, Energy Solutions, 740 Osborn Rd., Barnwell, SC 29812. E-mail: bssmith@energysolutions.com

[5]Laboratory Manager, Geological Engineering, Univ. of Wisconsin, Madison, WI 53706. E-mail: wang1@cae.wisc.edu

Note. This manuscript was submitted on August 8, 2016; approved on March 9, 2017; published online on May 31, 2017. Discussion period open until October 31, 2017; separate discussions must be submitted for individual papers. This paper is part of the ***Journal of Geotechnical and Geoenvironmental Engineering***, © ASCE, ISSN 1090-0241.

Table 1. Specification and Properties of As-Built Soil Barrier Layer

Property	Method	Specification	As-built[a]
Soil classification	ASTM D2487 (ASTM 2011a)	SM, ML, SC, CL, or CL-ML	SC
Saturated hydraulic conductivity (m/s)	ASTM D2434 (ASTM 2006b)	$\leq 5 \times 10^{-7}$	2.7×10^{-7} (5.0×10^{-8} to 4.4×10^{-7}; $n = 8$)[b]
Dry unit weight (pcf)	ASTM D698 (2007d)	≥92% of max by standard Proctor[c]	105.0 (101.0–111.9; $n = 12$)
Percent compaction (%)[d]		≥92%	95.6 (92.0–101.3; $n = 59$)
Water content (%)		0–5% ≥ OMC by standard Proctor[e]	18.1 (14.0–21.4; $n = 59$)
Plasticity index	ASTM D4318 (ASTM 2005b)	Not specified	39 (24–55; $n = 12$)[b]
Liquid limit		Not specified	63 (45–85; $n = 12$)[b]

[a]Data from construction field density soil tests unless otherwise specified; data are in format: mean (minimum to maximum; n = number of samples).
[b]Data from hydraulic conductivity tests on specimens from thin-wall sampling tubes.
[c]Maximum dry density by standard Proctor ranged from 107.8 to 110.5 lb/ft^3.
[d]Relative to maximum unit weight by standard Proctor.
[e]OMC = optimum moisture content; OMC ranged from 12.9 to 18.3%.

Table 2. Specifications and Properties of As-Built Geosynthetic Clay Liner (GCL)

Property	Method	Specification	As-built[a]
Bentonite loading (kg/m^2)	ASTM D5261 (ASTM 2010b)	≥3.9[b]	5.1 (5.0–5.2; $n = 65$)
Top geotextile (g/m^2)		≥225[c]	268 (249–317; $n = 65$)
Bottom geotextile (g/m^2)		≥110[d]	112 (112–112; $n = 65$)
Permeability (m/s)	ASTM D5084 (ASTM 2003)	$\leq 4 \times 10^{-11}$ m/s	5×10^{-12} (4×10^{-12} to 7×10^{-12}; $n = 32$)[e]
Swell index (mL/2 g)	USP NF XVII	≥25	27.9 (31.0–26.0; $n = 65$)
Moisture content (%)	ASTM D4643 (ASTM 2017)	Not specified	8.4 (7.4–9.8; $n = 65$)

[a]Data from manufacturer quality control tests unless otherwise specified; data are in format: mean (minimum to maximum; n = number of samples).
[b]30 Mesh, natural sodium bentonite from Wyoming.
[c]Style 205B nonwoven polypropylene fabric; specification is for minimum average value.
[d]Style 60 Tex woven polypropylene fabric; specification is for minimum average value.
[e]Data from manufacturer flexible wall hydraulic conductivity tests with distilled water, cell pressure = 345 kPa, head pressure = 310 kPa, and tail pressure = 276 kPa.

Table 3. Specifications and Properties of As-Built Geomembrane (GM)

Property	Method	Specification	As-built[a]
Tensile yield strength [MD (kN/m)]	ASTM D638 (ASTM 2014b)	≥22.9	26.7 (24.9–29.4; $n = 171$)
Tensile yield strength [TD (kN/m)]			27.6 (24.2–30.6; $n = 171$)
Elongation at tensile yield [MD (%)]		≥13.0	17.3 (14.2–22.0; $n = 171$)
Elongation at tensile yield [TD (%)]			16.4 (13.6–24.0; $n = 171$)
Melt flow index (g/10 min)	ASTM D1238 (ASTM 2004b)	—	0.27 (0.25–0.33; $n = 15$)
Carbon black (%)	ASTM D1603 (ASTM 2014a)	2.0–3.0	2.5 (2.3–2.7; $n = 171$)
Thickness (mm)	ASTM D751 (ASTM 2011b)	≥1.52	1.55 (1.52–1.68; $n = 174$)

Note: MD = machine direction; TD = transverse direction.
[a]Data from conformance and manufacturers quality assurance testing; data are in format: mean (minimum to maximum; n = number of samples).

conductivity and water content; samples of the soil barrier also were tested for dry density, and samples of the GCL were tested for soluble cations (SC), bound cations (BC), cation exchange capacity (CEC), and swell index (SI). Samples of the geomembrane were tested for melt flow index (MFI), oxidative induction time (OIT), tensile properties, and stress crack resistance (SCR). Results of the tests show the status of the cover materials, which reflect the influence of age in the near surface environment (14 years in service), combined with differential settlement (determined to warrant repair after approximately 13.5 years in service).

Exhumation and Field Observations

Differential settlement of the cover was observed in an area approximately 5 × 10 m (Figs. 1 and 2) after the cover had been in service for approximately 13.5 years. Along the periphery of a disposal trench (SCDHEC 2007), the vertical displacement was approximately 0.3 m over approximately 0.4 m horizontal (Figs. 2 and 3); this region, between the top and bottom of differential settlement, was the area of maximum distortion in the cover components. The barrier layers were sampled following careful removal of the overlying cover soils. Samples were collected from the geomembrane, GCL, and the soil barrier layer.

Sampling details are provided in the subsequent sections. Samples were collected from the differentially settled region and from an adjacent unsettled area (reference samples). Block samples of the undisturbed soil barrier were collected from above (BS6), within (BS3), and below (BS4) the area of maximum distortion shown in Fig. 3. Geosynthetic clay liner samples were collected above (GCL3a, b) and below (GCL4a, b) the area of maximum distortion. A geomembrane sample was collected from across the area of maximum distortion and from the settled area (GM2).

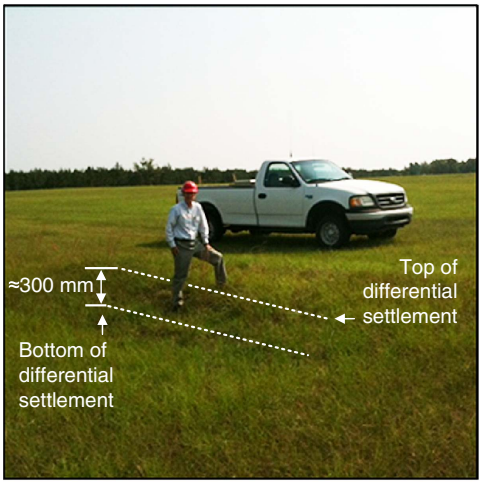

Fig. 1. Settlement feature before exhumation (image by William Albright)

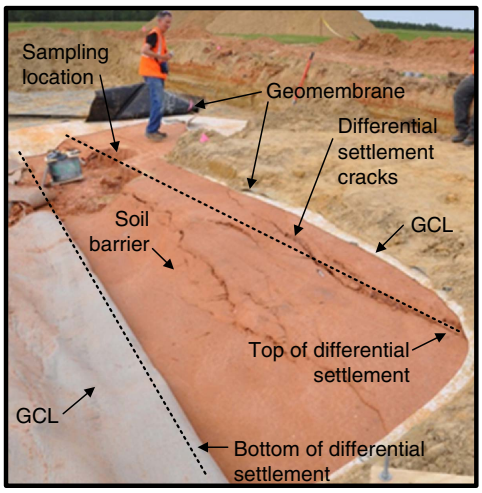

Fig. 2. Exposed soil barrier layer along boundary of trench in which differential settlement occurred; samples collected from geomembrane, GCL, and soil barrier (image by Joseph Scalia IV)

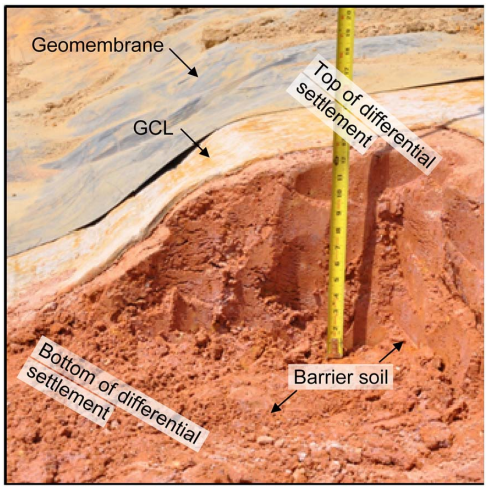

Fig. 3. Differential settlement of barrier system; geomembrane, GCL, and soil barrier layer following removal of surface soil and sand drainage layers (image by Joseph Scalia IV)

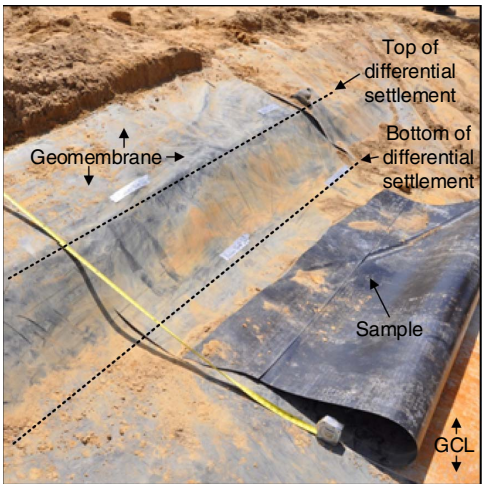

(a)

(b)

Fig. 4. Geomembrane samples from areas: (a) disturbed; (b) undisturbed by differential settlement; photograph (b) shows sampling location (GM3) with wrinkle in the geomembrane (images by Joseph Scalia IV)

Geomembrane Exhumation

Samples of the geomembrane were obtained from areas affected and unaffected by differential settlement. Exhumed samples of geomembrane in both settled and unsettled areas showed no visual evidence of breach or strain (e.g., tearing). One sample (GM1) was obtained from an undisturbed area approximately 5 m outside the settled region; two samples (GM2a and GM2b) were obtained within the area of maximum distortion between the top and bottom of differential settlement [Fig. 4(a)], and one sample (GM3) from the flat portion of the settled region. Sample GM3 included a wrinkle [Fig. 4(b)] and a section of dual-track fusion seam. Samples were removed by cutting the perimeter with a sharp utility knife. Geomembrane samples were rolled, wrapped in plastic, and shipped to TRI Environmental, Inc. (TRI) in Austin, Texas for analysis.

Geosynthetic Clay Liner Exhumation

The GCL showed no visual evidence of damage in or around the settled area. The GCL panel overlaps parallel and perpendicular to the long axis of maximum cover distortion showed no visual

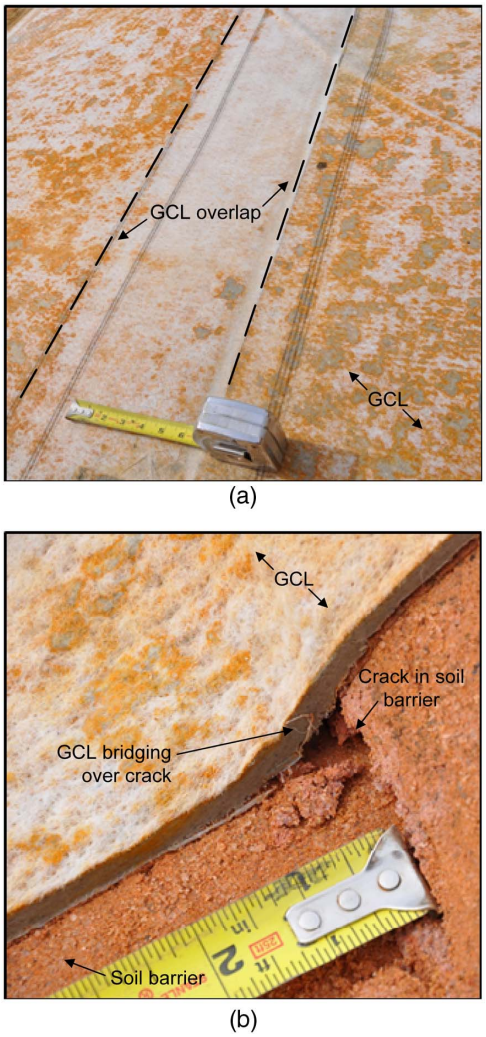

Fig. 5. (a) GCL overlap above and parallel to differential settlement; (b) GCL bridging crack in soil barrier layer (crack running parallel to axis of maximum cover distortion) (images by Joseph Scalia IV)

signs of shifting (distortion, smearing of bentonite, or mineral precipitation) as illustrated in Fig. 5(a). The GCL bridged over cracks in the soil barrier layer [Fig. 5(b)], and there was no visual evidence of bentonite cracking in the areas of maximum distortion, consistent with the laboratory-based findings reported by LaGatta et al. (1997).

Samples of GCL were collected to represent areas away from the settlement, immediately above the area of maximum distortion, immediately below the area of maximum distortion, and in a flat area that had settled uniformly. Sampling the GCL was conducted after removal of the geomembrane and using the procedures described in ASTM D6072 (ASTM 2009). The perimeter of each GCL sample (0.3×0.3 m) was scored and cut with a razor knife while the GCL remained on the soil barrier layer. The GCL surrounding the sample was pulled back, and a rigid PVC plate (0.3×0.3 m) was slid under the sample as described in Scalia and Benson (2011). The GCL sample was wrapped with plastic sheeting to prevent loss of moisture, placed in plastic tubs, and covered with approximately 0.2 m of loose soil for protection during transport and storage. Samples were shipped to the geological engineering laboratories at the University of Wisconsin-Madison for analysis.

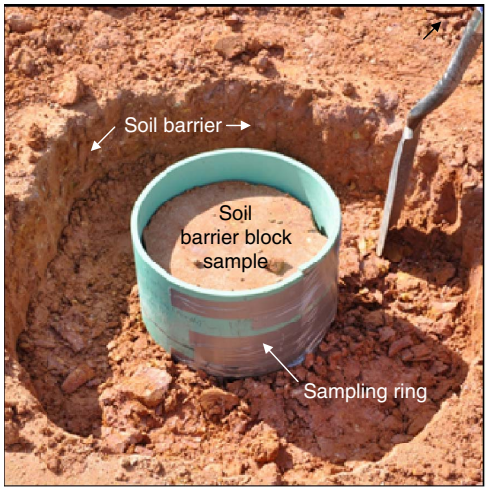

Fig. 6. Sampling of large undisturbed soil block (BS5) from intact area (reference sample); photo shows how surrounding soil is removed and the PVC ring is gradually slipped over sample (image by Joseph Scalia IV)

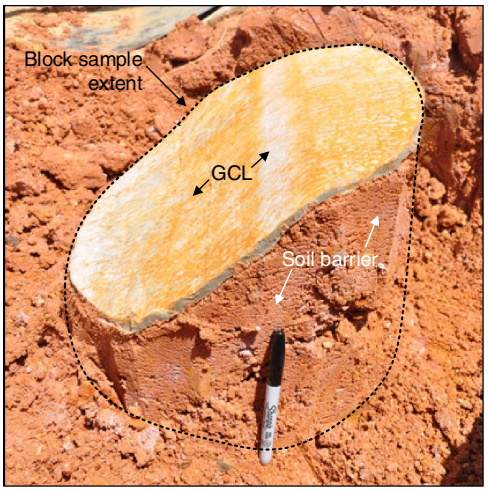

Fig. 7. Sampling of GCL and underlying soil in disturbed area (BS3); photo shows sample collected from area of settlement distortion and includes soil barrier layer and overlying GCL (image by Joseph Scalia IV)

Soil Barrier Layer

Samples of the soil barrier layer were collected as large blocks using the procedure in ASTM D7015 (ASTM 2007a; Fig. 6). All block samples were trimmed into PVC rings with a diameter of 365 mm. Both ends of the sample were sealed with plastic sheeting and the sample was secured between wooden endplates during transport. All samples were stored in a 100% humidity room prior to testing.

One of the block samples from the distorted area was collected with the overlying GCL in place (BS3; Fig. 7). The GCL sample was manually trimmed with a razor knife and the surrounding GCL was pulled back, prior to soil block sampling (Fig. 7). Once inside the PVC sampling ring, the GCL was covered by plastic sheeting to prevent moisture loss. The void space between the GCL and the top endplate was filled with soil to protect the sample during transport.

Samples were shipped to the geological engineering laboratories at the University of Wisconsin-Madison for analysis.

Laboratory Methods

Geomembrane

Polymer Properties

Standard oxidative-induction time (Std-OIT) and high pressure (HP) OIT were measured by the procedures in ASTM D3895 (ASTM 2007c) and ASTM D5885 (ASTM 2006a). Original design specifications and the measured as-built properties did not include OIT or HP-OIT. As of 2015, Std-OIT ≥100 min and HP-OIT ≥400 min are specified in GRI-GM13 (Geosynthetic Institute 2011) for a new smooth 1.5-mm geomembrane.

Melt flow index was measured following ASTM D1238 (ASTM 2004b). Original design specifications did not include MFI; however, MFI was measured for the as-built geomembranes (Table 3).

Stress crack resistance was measured by the notched constant tensile load environmental stress crack resistance test (NCTL-ESCR) in ASTM D5397 (ASTM 2007b). Stress crack resistance is reported in hours to failure. Reductions in SCR are indicative of transition to a more brittle structure resulting from polymer degradation (chain scission reactions; Rowe and Sangam 2002) of amorphous inter-crystalline domain polymer chains (Hsuan 2000). Original design specifications and measured as-built properties did not include NCTL-ESCR. As of 2015, SCR ≥ 500 h is specified in GRI-GM13 for new smooth 1.5-mm HDPE geomembrane (Geosynthetic Institute 2011).

Tensile strength was measured following ASTM D6693 (ASTM 2004a). As with SCR, changes in tensile strength are indicative of changes in the polymer; tensile strength decreases when the SCR decreases (Koerner 2012). Original design specifications included tensile yield strength ≥22.9 kN/m, and elongation at tensile yield ≥13.0% (Table 3). As of 2015, a yield strength ≥22 kN/m and yield elongation ≥12% is specified in GRI-GM13 for a new smooth 1.5-mm HDPE geomembrane (Geosynthetic Institute 2011), which is similar to, but slightly lower than, the original design specifications.

Seam peel strength and shear strength were measured on Sample GM3 following ASTM D6392 (ASTM 2008). Specimens were taken from five points along the seam sample. Original design specifications included seam peel strength ≥15.6 kN/m and seam shear strength ≥22.9 kN/m (Table 3). As of 2015, a peel strength ≥15.9 kN/m and shear strength ≥21.0 kN/m are specified in GRI-GM19 (Geosynthetic Institute 2015) for a HDPE geomembrane hot wedge seam, comparable to the original design specifications. The wrinkle and seam also were examined for microcracks using an optical microscope.

Geosynthetic Clay Liner

Saturated hydraulic conductivity of each GCL sample was measured in general accordance with the procedure in ASTM D5084 (ASTM 2003) Method B (falling head, constant tailwater elevation). Tests were conducted on specimens trimmed to a diameter of 152 mm at an average effective stress of 18 kPa without backpressure, and with a hydraulic gradient between 160 and 230. The effective stress was selected to simulate the state of stress in the cover. The hydraulic gradient used is high relative to hydraulic gradients used for testing soils, but is typical for testing GCLs (Shackelford et al. 2000), which are much thinner than typical soil specimens used in hydraulic conductivity tests. The permeant liquid was average water (AW) as defined in Scalia and Benson (2010a), which consists of 1.3 mM sodium chloride (NaCl) and 0.8 mM calcium chloride ($CaCl_2$), and represents average soil pore water. In addition, three replicate specimens were permeated with standard water (SW) (10 mM $CaCl_2$) for a comparison with data from Meer and Benson (2007) and Scalia and Benson (2011). Design specifications required a hydraulic conductivity $\leq 5 \times 10^{-11}$ m/s (Table 2). Swell index, in situ water content, SC, BC, and CEC were measured on trimmings remaining from preparation of the specimens for hydraulic conductivity testing. Design specifications required a SI ≥ 25 mL/2 g (Table 2).

Swell index tests were conducted in accordance with the procedure in ASTM D5890 (ASTM 2006c) using deionized water as the hydrating solution.

Tests for SC, BC, and CEC were performed on the bentonite in each GCL sample in accordance with ASTM D7503 (ASTM 2010a) to determine the degree of cation exchange. Chemical analyses of extracts for SC and BC were conducted using inductively coupled plasma optical emission spectroscopy (ICP-OES) following the U.S. Environmental Protection Agency (EPA) Method 6010 B (USEPA 2007) and the quality control procedures in USEPA SW-846 (USEPA 2007).

Bound cation mole fractions were calculated as the ratio of total charge per unit mass of bentonite associated with a particular cation to the CEC. Concentration and relative abundance of SC were quantified by the total SC charge per mass (TCM) and the monovalent-to-divalent ratio (MDR) (Scalia and Benson 2010a). The TCM is defined as the total charge of monovalent and divalent SC per mass of soil solid. The MDR is defined as the ratio of the total charge of monovalent SC per mass relative to the total charge of divalent SC per mass. These bentonite-mass-based metrics are analogous to the ionic strength and ratio of MDR cations (RMD) used to describe permeant waters (Kolstad et al. 2004). Design specifications did not include requirements for SC or BC.

Water content of bentonite from GCL samples was determined following the methods in ASTM D2216 (ASTM 2005a). Geotextiles were not included in the water content measurements.

Soil Barrier Layer

Saturated hydraulic conductivity of the soil barrier was measured using flexible-wall permeameters following the procedure in ASTM D5084 (ASTM 2003) Method C (falling head, rising tailwater elevation). All tests were conducted at an effective stress of 19 kPa using a backpressure of 210 kPa, and a hydraulic gradient of 10 to simulate field conditions. Block samples were trimmed into cylindrical specimens for hydraulic conductivity testing having a diameter of 305 mm and height of 180 mm. Water content was measured on the trimmings, and unit weight of the cylindrical specimen was determined from the mass and volume. Design specifications required the soil barrier to have a hydraulic conductivity $\leq 5 \times 10^{-7}$ m/s (Table 1).

Three block samples contained cracks (BS2, BS3, and BS6). In the laboratory, the cracks were filled with well-graded sand prior to removal from sampling rings to ensure the soil structure was maintained during hydraulic conductivity testing (Fig. 8). Care was taken to prevent crack disturbance (opening) during trimming and assembly in the flexible wall permeameter.

One of the block samples collected from the distorted area that contained cracks also was overlain by a GCL (BS3; Fig. 7). This specimen was trimmed and tested as a composite sample (GCL over soil barrier) to determine the composite hydraulic conductivity. When installing this specimen in the permeameter, the

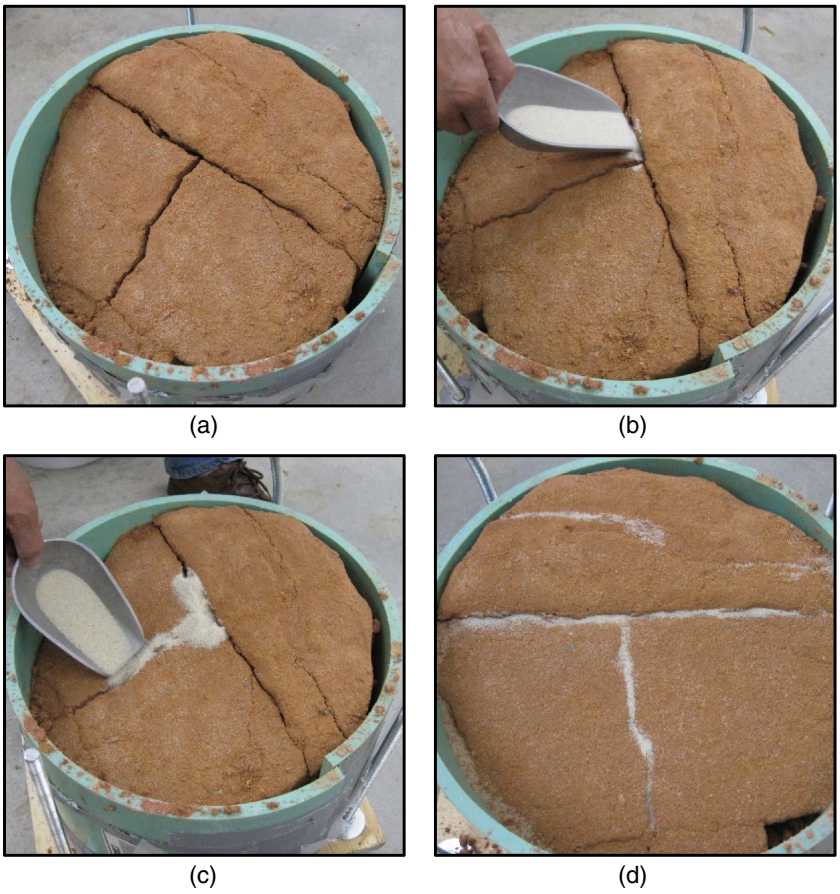

Fig. 8. Preparation of block sample containing cracks for hydraulic conductivity testing in flexible wall permeameter: (a) original block sample in sampling ring; (b and c) filling with well-graded sand; (d) surface of block sample with sand-filled cracks prior to trimming (images by Joseph Scalia IV)

GCL was overlain by pea gravel to create a horizontal surface on which to place the top cap of the permeameter. Prior to placing pea gravel, the specimen [Fig. 9(a)] was surrounded by a flexible membrane [Fig. 9(b)] and a rigid sheath of perforated sheet metal secured with hose clamps. The sheath provided the rigidity necessary to retain the pea gravel placed above the GCL. A thin layer of bentonite paste (i.e., natural sodium bentonite hydrated in AW) was applied around the perimeter of the GCL specimen before placing the pea gravel to prevent gravel particles from penetrating the GCL sidewall around the periphery of the GCL [Fig. 9(c)]. The GCL was topped with pea gravel [Fig. 9(d)] and permeated with the perforated rigid sheath in place to retain the gravel until the confining pressure was applied.

Results and Implications

Geomembrane

Properties of geomembrane samples are shown in Table 4. Thickness of the 1.5-mm geomembrane was measured at multiple points including the point of maximum distortion caused by differential settlement and at locations more distant from the maximum distortion. Measurements of the geomembrane thickness at points near the area of maximum distortion showed the geomembrane thinned slightly (<3.5% or <0.05 mm) under stress from differential settlement.

Tensile Strength

Tensile strength of the exhumed geomembrane is summarized in Table 4. Four of the five samples had significant scratches (possibly the result of exhumation activities) that may have affected the tensile strength. When tested, specimens typically break at the most significant flaw; scratches incurred during installation (or exhumation) often are the critical feature (Koerner 2012). Tensile yield strengths (Table 4) exceed the original design specifications (Table 3; viz tensile yield strength $\geq$22.9 kN/m, elongation at tensile yield $\geq$13.0%), and are indistinguishable from the range of properties reported for the as-built condition (Table 3; machine and transverse direction were not recorded for the exhumed samples and, therefore, cannot be differentiated). The lack of reduction in tensile strength suggests that the geomembrane was still within Stage A (antioxidant depletion period) of geomembrane aging as defined by Hsuan and Koerner (1998) and Rowe and Sangam (2002). This inference is further supported by OIT $>$ 0 min as discussed subsequently.

Stress Crack Resistance

The SCR of the geomembrane samples is reported in Table 4. The mean SCR ranged between 561 and $>$800 h, which is longer than the current minimum requirement of 500 h specified by GRI-GM13 (Geosynthetic Institute 2011). The SCR was not specified in the design specifications, nor reported for as-built conditions. No systematic trend in SCR was apparent between the reference, stressed, and settled areas.

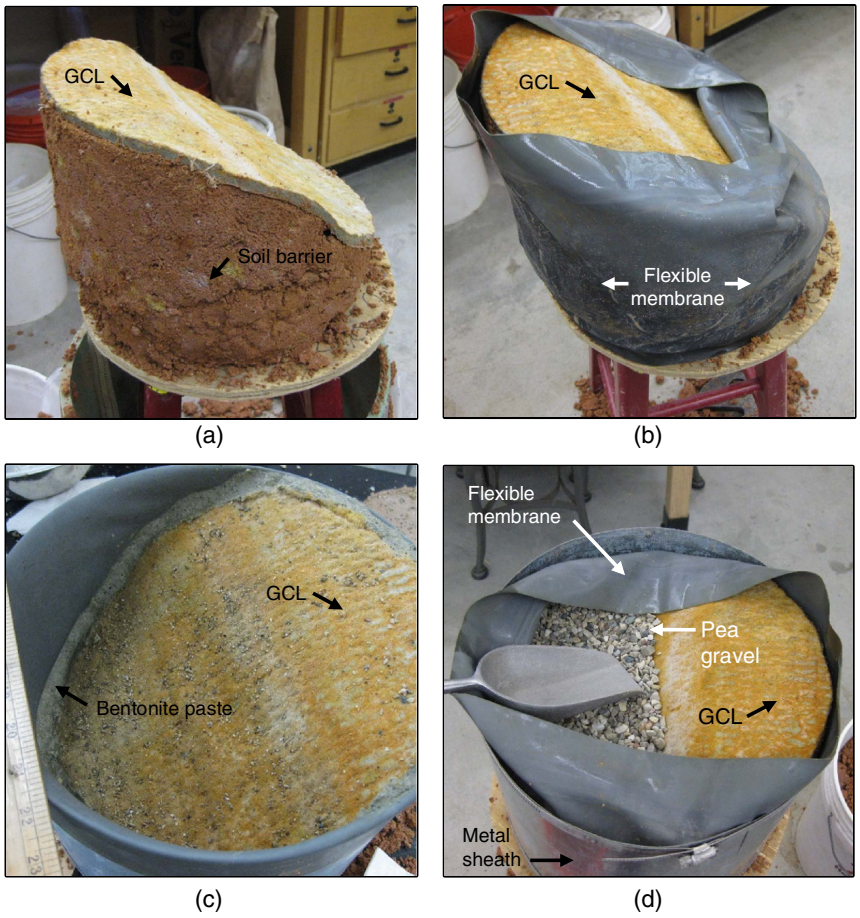

Fig. 9. Preparation of block sample overlain with GCL for hydraulic conductivity testing in flexible wall permeameter; (a) trimmed specimen; (b) specimen surrounded by flexible membrane; (c) bentonite paste applied around periphery of GCL; (d) pea gravel over GCL for permeameter end cap (images by Joseph Scalia IV)

Table 4. Oxidation Induction Time (OIT), High-Pressure Oxidation Induction Time (HP-OIT), Melt Flow Index (MFI), Tensile Strength, and Notched Constant Tensile Load Environmental Stress Crack Resistance (NCTL-ESCR) for Geomembrane Samples; Stressed Samples Removed from Distortion Cusp; Settled Samples Removed from Flat Area That Had Settled

Sample	OIT (min)	HP-OIT (min)	MFI (g/10 min)[a]	Tensile yield strength[b] (kN/m)	Elongation at tensile yield[b] (%)	NCTL-ESCR[b] (h)
GM1	120	295	0.31 (0.30–0.31)	29.1 ± 1.5	17 ± 0	541 ± 44
GM2a (stressed)	110	294	0.29 (0.29–0.29)	30.0 ± 1.1	17 ± 0	>800
GM2b (stressed)	113	303	0.31 (0.28–0.34)	29.5 ± 1.3	17 ± 1	659 ± 100
GM2a (settled)	113	309	0.32 (0.38–0.28)	28.0 ± 0.1	20 ± 0	>800
GM2b (settled)	110	311	0.28 (0.28–0.29)	28.7 ± 0.4	17 ± 0	>668 (3/5 broken)

[a]Average of 2 tests.
[b]Average of 5 tests.

Peel Strength

Results of peel strength and shear strength tests on the hot-wedge seam from sample GM3 are reported in Table 5. The peel strength and shear strength exceeded original design specifications (viz peel strength ≥15.6 kN/m, and shear strength ≥22.9 kN/m; Table 3) and current standard specifications (i.e., GRI-GM19; Geosynthetic Institute 2015) for a 1.5-mm geomembrane (viz peel strength = 15.9 kN/m; shear strength = 21.0 kN/m). Visual evaluation of the seam and the folded crease by optical microscope showed no microcracks.

Polymer Degradation

Oxidation induction time for geomembranes is indicative of the total amount of antioxidant in the geomembrane, and is summarized for the exhumed samples in Table 4. The OIT is the first property to change during the service life of a geomembrane, and approaches zero (or a residual OIT) before changes in mechanical properties become evident (Koerner 2012). The OIT for all samples exceeded 100 min (Table 4), the required minimum OIT for new geomembranes in the GRI-GM13 standard specifications (Geosynthetic Institute 2011). These data were consistent with the lack of

Table 5. Properties of Dual Track Wedge Welded Seams

Specimen	Peel strength (kN/m) Side A	Peel strength (kN/m) Side B	Shear strength (kN/m)	% Peel
1	20.3	18.9	27.0	0
2	21.0	21.1	27.7	0
3	21.8	22.2	27.7	0
4	19.9	20.4	27.4	0
5	19.4	22.3	27.7	0
Average	20.4	21.0	27.5	0
SD	0.9	1.4	0.3	0
COV (%)	4.60	6.70	1.10	0

Note: COV = coefficient of variation; SD = standard deviation.

measurable decrease in geomembrane tensile strength. For all samples, the variability in measured Std-OIT and in HP-OIT was small. The relative standard deviation for both OITs is <4%, supporting that antioxidants were depleted uniformly despite differential settlement.

Lack of as-built Std-OIT or HP-OIT measurements prevented back-calculating the extent of antioxidant depletion that had occurred within the geomembrane since installation. However, the time to Std-OIT depletion can be extrapolated assuming published Std-OIT depletion rates are approximately representative of the installed geomembrane by using the first-order OIT depletion model defined by Hsuan and Koerner (1998)

$$\ln(\text{OIT}) = \ln(P) - (S)(t) \quad (1)$$

where OIT = OIT time (min), taken to be 0.5 min for standard OIT (the time at which essentially all antioxidants in the geomembrane are consumed), and 20 min for HP-OIT; S = OIT depletion rate (min/month), assumed ≈0.00212 for Std-OIT tests and ≈0.000909 for HP-OIT tests-based data scaled to 20°C reported by Hsuan and Koerner (1998); t = time (months); and P = measured value of OIT for the geomembrane. Combining Eq. (1) and the measured OIT data presented in Table 4, the time for essentially all antioxidants in the geomembrane to be consumed was on the order of 212–215 years; combining Eq. (1) and the HP-OIT data presented in Table 4, a range of approximately 246–251 years was calculated for complete antioxidant depletion. These times are only approximations, as the assumed Std-OIT depletion rates may not represent field conditions precisely. Nevertheless, these predictions provide a baseline for future comparisons.

Melt flow index was measured to provide an indirect measure of changes in polyethylene molecular weight. The MFI data are reported in Table 4. Measured MFI (0.28–0.32 g/10 min) were similar to the as-built condition (0.25–0.33 g/10 min). Oxidation and other degradation mechanisms resulted in lower molecular weight and higher MFI (Koerner 2012). There was no standard MFI for geomembranes. The MFI measured in this study served three purposes: (1) to compare with as-built MFI, (2) to compare geomembrane samples from areas distorted by settlement and undistorted areas, and (3) to establish a baseline for future comparison. The MFI ranged between 0.28 and 0.32 g/10 min (Table 4), within the range (0.25–0.33 g/10 min) reported for the as-built condition (Table 3). Soil particles trapped on the exhumed samples also may have affected the MFI of the exhumed samples. The MFI did not indicate any significant changes to the geomembrane associated with differential settlement.

Table 6. Water Content, Swell Index, and Saturated Hydraulic Conductivity to Average Water (AW) and Standard Water (SW) of Exhumed GCLs

Sample	Sampling location	Water content (%)	Permeant liquid	Hydraulic conductivity (m/s) $\times 10^{-12}$
GCL1a	Away from settlement	112.2	AW	9.6
			SW	1.5
GCL1c	Away from settlement	115.0	AW	8.6
			SW	7.9
GCL2a	Away from settlement	110.4	AW	9.5
GCL2c	Away from settlement	119.6	AW	7.0
			SW	8.5
GCL3a	Above distortion cusp	102.6	AW	8.6
GCL4a	Below distortion on flat	129.4	AW	9.0
GCL4b	Below distortion cusp	151.5	AW	8.6

Geosynthetic Clay Liner

Hydraulic conductivities of the GCL samples are summarized in Table 6 along with the water contents when exhumed. Swell indices of the bentonite are shown in Table 7 with the CEC and the distribution of SC and BC. All of the hydraulic conductivities were $<1 \times 10^{-11}$ m/s (Table 6), which is lower than the hydraulic conductivity normally associated with a new GCL (typically $1–3 \times 10^{-11}$ m/s) (Petrov and Rowe 1997; Shackelford et al. 2000; Scalia and Benson 2011), and less than the design specification for hydraulic conductivity ($\leq 4 \times 10^{-11}$ m/s). Hydraulic conductivities measured on the exhumed GCLs cannot be directly compared with hydraulic conductivity of the as-built GCLs measured using distilled water (Table 2) because of differences in permeant water chemistry that can significantly impact the hydraulic conductivity of GCLs exhumed from composite covers (Scalia and Benson 2010a).

The GCLs had exhumed water contents in excess of 100%, indicating that the bentonite was well hydrated and in an osmotic state (Scalia and Benson 2011). Meer and Benson (2007) showed

Table 7. Soluble Cations, Bound Cations, and Cation Exchange Capacity (CEC) of GCLs

Sample	Soluble cations ($cmol^+/kg$) Na^+	K^+	Ca^{2+}	Mg^{2+}	Bound cations (molar ratio) Na^+	K^+	Ca^{2+}	Mg^{2+}	Swell index (mL/2g)[a]	CEC ($cmol^+/kg$)
GCL1a	2.0	0.0	0.2	0.1	0.41	0.01	0.46	0.12	24.0	69.5
GCL1c	2.2	0.0	0.2	0.1	0.42	0.02	0.45	0.11	21.5	70.3
GCL2a	2.0	0.0	0.2	0.1	0.41	0.01	0.46	0.12	21.0	69.4
GCL2c	2.6	0.0	0.3	0.1	0.42	0.02	0.45	0.11	23.9	66.1
GCL3a	1.5	0.0	0.2	0.2	0.38	0.01	0.47	0.13	22.0	69.6
GCL4a	1.7	0.0	0.4	0.3	0.39	0.01	0.47	0.12	24.5	70.5
GCL4b	1.4	0.0	0.2	0.2	0.37	0.02	0.48	0.13	22.5	70.1

[a]Average of 4 tests.

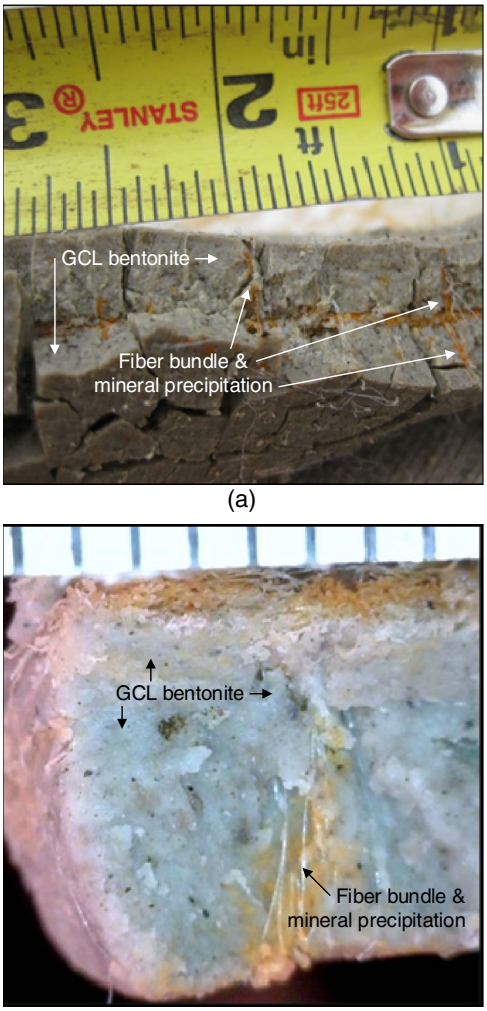

Fig. 10. (a) Cross-section of GCL during exhumation (b) and after permeation; scale in top photo in mm; mineral precipitation is visible along needle punching fiber bundle in (b) (images by Joseph Scalia IV)

that GCLs with exhumed water content >100% retained low-hydraulic conductivity when in service. These findings corroborated the hypothesis proffered by Scalia and Benson (2011) that a GCL placed on sufficiently moist subgrade and overlain with a geomembrane will maintain a swollen structure and corresponding low-hydraulic conductivity to dilute permeant solutions.

The low-hydraulic conductivity of sodium bentonite is a result of swelling of the bentonite that occurs in two phases: the crystalline phase and the osmotic phase (Norrish and Quirk 1954). Osmotic swelling can produce far greater swell than crystalline swelling alone, and is responsible for the high-swelling capacity and low-hydraulic conductivity of GCLs with sodium bentonite. Replacement of sodium by divalent cations reduces osmotic swell and results in increased hydraulic conductivity (Jo et al. 2001, 2004). A new GCL typically has bentonite with a swell index of approximately 30 mL/2 g and Na^+ as the predominant bound cation (Shackelford et al. 2000; Scalia and Benson 2011); the as-built GCL had a mean swell index = 27.9 mL/2 g. The exhumed GCLs had swell indices ranging from 21.0 to 24.5 mL/2 g (< the design standard of 25 mL/2 g), and comparable molar ratios of bound sodium ion (Na^+) and calcium ion (Ca^{2+}) cations (Table 7). The reduction in swell index and increased presence of Ca^{2+} are indicative of cation exchange within the bentonite. However, cation exchange apparently had no adverse effect on the hydraulic conductivity of the GCL (Table 7). The minimal reduction in swell index, and maintenance of a greater than 0.35 bound sodium mole fraction, despite 14 years in service, is inconsistent with the trends of lower swell index, and lower-bound sodium mole fractions, with increased exhumed water content for composite cover GCLs shown by Scalia and Benson (2011). One possible hypothesis for this deviation may be differences between the soil barrier layer pore water chemistry in this study and those evaluated by Scalia and Benson (2011). Unfortunately, pore water chemistry was not determined as part of this study and, thus, data are unavailable to test this hypothesis.

The CEC of the bentonite ranged between 66.1 and 70.5 $cmol^+/kg$ (Table 7), which is consistent with the CEC of new bentonite (Scalia and Benson 2011) and suggests that no change in bentonite mineralogy occurred while the GCL was in service.

Mineral precipitation was visible in all samples along the needle-punching fiber bundles (Fig. 10). Similar mineral precipitation was reported by Scalia and Benson (2010b) for GCLs exhumed from composite barriers in a final cover over a municipal solid waste (MSW) landfill. Scalia and Benson (2010b) showed that preferential flow occurred along these fiber bundles when the exhumed GCLs were permeated with SW, but not when permeated with AW or deionized water. Specimens from three GCL samples were permeated with SW to investigate the potential for preferential flow concurrent with stained needle-punching fiber bundles. Preferential flow along stained fiber bundles was not observed in the GCLs exhumed in this study. All of the GCLs had low-hydraulic conductivity (7.9×10^{-12} to 1.5×10^{-11} m/s) to SW, and similar hydraulic conductivity to AW (7.0×10^{-12} to 9.6×10^{-12} m/s; Table 6). The GCL appears to have preferentially hydrated along the needle-punching fiber bundles similar to the process described by Scalia and Benson (2010b), but attained sufficient swell to seal off these pathways.

Soil Barrier Layer

Hydraulic conductivities of the block samples from the soil barrier are summarized in Table 8. Except for sample BS3

Table 8. Properties of Block Samples Exhumed from Soil Barrier Layer

Sample	Sampling location	Notes	Gravimetric water content (%)	Dry unit weight (pcf)	Hydraulic conductivity (m/s)
BS1	Away from distortion	Reference sample	15.2	113.6	2.2×10^{-7}
BS2	Away from distortion	Contains small cracks	16.0	113.6	1.5×10^{-7}
BS3	Middle of distortion	Contains large crack and GCL	ND	ND	8.4×10^{-10}
BS4	Bottom of distortion	—	13.2	114.2	4.7×10^{-7}
BS5	Away from distortion	Reference sample	14.0	116.7	1.1×10^{-7}
BS6	Top of distortion	Contains large crack	14.0	ND	3.0×10^{-6}

Note: ND = not determined. Specimens fragile because of cracks.

(shown in Figs. 7 and 9), which was permeated as a composite sample with an overlying GCL layer, the hydraulic conductivities ranged between 1.1×10^{-7} and 3.0×10^{-6} m/s. When samples with cracks are excluded, the hydraulic conductivity fell in the narrow range of 1.1×10^{-7} to 4.7×10^{-7} m/s.

Outside the area of significant cracking, the hydraulic conductivity of the soil barrier met the original specification of $\leq 5 \times 10^{-7}$ m/s, and was within the range reported for the as-built condition. Cracks within the area of disturbance increased the soil hydraulic conductivity by an order of magnitude, exceeding the design specification.

The block sample overlain with a GCL had a lower hydraulic conductivity (8.4×10^{-10} m/s) than the other samples, which is ascribed to the low-hydraulic conductivity of the GCL. The GCL was effective in bridging over cracks (Fig. 4) and moderating flow despite having been distorted by settlement.

Summary and Conclusions

Properties of earthen and geosynthetic barrier materials exhumed from a conventional cover with a composite barrier are presented, providing conditions after 14 years of service. Samples of the barrier materials were exhumed during repair activities in an area in which differential settlement occurred after approximately 13.5 years of service. Samples were collected from a HDPE geomembrane, GCL, and a soil barrier. Testing was conducted on each material to assess the effects of age and differential settlement. Results were compared with as-built properties, design specifications, and when no design specification existed, contemporary standard specifications.

Tensile properties of the geomembrane and geomembrane seam met or exceeded current specifications for new material (tensile yield strengths $\geq$28.0 kN/m and elongation at tensile yield $\geq$17%). Stress crack resistance also exceeded the specification for new material. Oxidation induction time tests, used to assess the presence of chemicals added to the polymer to inhibit oxidative damage (i.e., antioxidants), yielded OIT $\geq$110 min, illustrating that antioxidants are present in quantities greater than standard specifications require for a new material (e.g., $\geq$100 min). There were no cracks in the geomembrane across the area of differential settlement. The absence of apparent damage to the geomembrane at the exhumed site suggests that larger disturbance is required to cause cracks in the HDPE. The geomembrane appeared to be functioning as intended.

Saturated hydraulic conductivity of all GCL samples fell within a narrow range ($7.0–9.6 \times 10^{-12}$ m/s), lower than the hydraulic conductivity normally associated with a new GCL at stresses in final covers (typically $1–3 \times 10^{-11}$ m/s), and less than the original design specifications ($<4 \times 10^{-11}$ m/s). Swell index and bound cation mole fractions showed evidence of partial cation exchange within the bentonite, with swell index decreasing from a mean of 27.9 mL/2 g as constructed to between 21.0 and 24.5 mL/2 g (< the design specification of 25 mL/2 g). However, the low-hydraulic conductivities indicated that the GCL was still an effective hydraulic barrier, meeting design specifications, even in areas in which the GCL had been distorted because of settlement. The GCL samples all had water content in excess of 100%, indicating the bentonite was in an osmotic-hydrated state associated with low-hydraulic conductivity irrespective of gradual cation exchange with a low concentration divalent-cation bearing solution.

Hydraulic conductivity of the soil barrier in areas unaffected by differential settlement ranged from 2.2×10^{-7} to 1.1×10^{-7} m/s, and met the design specification ($<5.0 \times 10^{-7}$ m/s). Settlement cracks in the soil barrier resulted in an order-of-magnitude increase in hydraulic conductivity, resulting in exceedance of the design specification. However, because the hydraulic conductivity of the overlying GCL was more than four orders of magnitude lower, cracking of the soil barrier is likely to have had a minimal impact on downward percolation through the combined soil barrier components (soil barrier and GCL) of the cover system because of the intact geomembrane and GCL barrier layers.

These findings provide insight into the long-term engineering behavior of barrier materials used for final covers. However, the results of this study are site specific and should not be generalized to other cover systems. More study of the in-service condition of final covers is recommended.

Acknowledgments

Financial support for this study was provided by Energy Solutions Inc. and the U.S. DOE Office of Environmental Management through the Consortium for Risk Evaluation with Stakeholder Participation (CRESP). The South Carolina Department of Health and Environmental Control is acknowledged for supporting this study during cover repair activities at the Site.

References

Adams, V., Gupta, D., and Smegal, J. (2009). "Lessons learned from independent technical review of U.S. Department of Energy low-level radioactive waste landfills/disposal facilities." *Proc., WM2009 Conf.*, WM Symposia, Inc., Tempe, AZ.

ASTM. (2003). "Standard test method for measurement of hydraulic conductivity of saturated porous materials using a flexible wall permeameter." *ASTM D5084*, West Conshohocken, PA.

ASTM. (2004a). "Standard test method for determining tensile properties of nonreinforced polyethylene and nonreinforced flexible polypropylene geomembranes." *ASTM D6693*, West Conshohocken, PA.

ASTM. (2004b). "Standard test method for melt flow rates of thermoplastics by extrusion plastometer." *ASTM D1238*, West Conshohocken, PA.

ASTM. (2005a). "Standard test method for laboratory determination of water (moisture) content of soil and rock by mass." *ASTM D2216*, West Conshohocken, PA.

ASTM. (2005b). "Standard test methods for liquid limit, plastic limit, and plasticity index of soils." *ASTM D4318*, West Conshohocken, PA.

ASTM. (2006a). "Standard test method for oxidative induction time of polyolefin geosynthetics by high-pressure differential scanning calorimetry." *ASTM D5885*, West Conshohocken, PA.

ASTM. (2006b). "Standard test method for permeability of granular soils (constant head)." *ASTM D2434*, West Conshohocken, PA.

ASTM. (2006c). "Standard test method for swell index of clay mineral component of geosynthetic clay liner." *ASTM D5890*, West Conshohocken, PA.

ASTM. (2007a). "Standard practices for obtaining intact block (cubical and cylindrical) samples of soils." *ASTM D7015*, West Conshohocken, PA.

ASTM. (2007b). "Standard test method for evaluation of stress crack resistance of polyolefin geomembranes using notched constant tensile load test." *ASTM D5397*, West Conshohocken, PA.

ASTM. (2007c). "Standard test method for oxidative-induction time of polyolefins by differential scanning calorimetry." *ASTM D3895*, West Conshohocken, PA.

ASTM. (2007d). "Standard test methods for laboratory compaction characteristics of soil using standard effort [12,400 ft-lbf/ft3 (600 kN-m/m3)]." *ASTM D698*, West Conshohocken, PA.

ASTM. (2008). "Standard test method for determining the integrity of nonreinforced geomembrane seams produced using thermos-fusion methods." *ASTM D6392*, West Conshohocken, PA.

ASTM. (2009). "Standard practice for obtaining samples of geosynthetic clay liners." *ASTM D6072*, West Conshohocken, PA.

ASTM. (2010a). "Standard test method for measuring exchangeable cations and cation exchange capacity of inorganic fine-grained soils." *ASTM D7503*, West Conshohocken, PA.
ASTM. (2010b). "Standard test method for measuring mass per unit area of geotextiles." *ASTM D5261*, West Conshohocken, PA.
ASTM. (2011a). "Standard practice for classification of soils for engineering purposes (unified soil classification system)." *ASTM D2487*, West Conshohocken, PA.
ASTM. (2011b). "Standard test methods for coated fabrics." *ASTM D751*, West Conshohocken, PA.
ASTM. (2014a). "Standard test method for carbon black content in olefin plastics." *ASTM D1603*, West Conshohocken, PA.
ASTM. (2014b). "Standard test method for tensile properties of plastics." *ASTM D638*, West Conshohocken, PA.
ASTM. (2017). "Standard test method for determination of water content of soil and rock by microwave oven heating." *ASTM D4643*, West Conshohocken, PA.
Benson, C., et al. (2011). "Engineered covers for waste containment: Changes in engineering properties & implications for long-term performance assessment." *NUREG/CR-7028*, Office of Research, U.S. Nuclear Regulatory Commission, Washington, DC.
Benson, C., Kucukkirca, E., and Scalia, J. (2010). "Properties of geosynthetics exhumed from a final cover at a solid waste landfill." *Geotext. Geomembr.*, 28(6), 536–546.
Geosynthetic Institute. (2011). "Standard specification for test methods, test properties and testing frequency for high density polyethylene (HDPE) smooth and textured geomembranes." *GRI Test Method 13*, Folsom, PA.
Geosynthetic Institute. (2015). "Standard specification for seam strength and related properties of thermally bonded polyolefin geomembranes." *GRI Test Method GM19*, Folsom, PA.
Hsuan, G. (2000). "Data base of field incidents used to establish HDPE geomembrane stress crack resistance specifications." *Geotext. Geomembr.*, 18(1), 1–22.
Hsuan, Y., and Koerner, R. (1998). "Antioxidant depletion lifetime in high density polyethylene geomembranes." *J. Geotech. Geoenviron. Eng.*, 10.1061/(ASCE)1090-0241(1998)124:6(532), 532–541.
Jo, H., Benson, C., and Edil, T. (2004). "Hydraulic conductivity and cation exchange in non-prehydrated and prehydrated bentonite permeated with weak inorganic salt solutions." *Clays Clay Miner.*, 52(6), 661–679.
Jo, H., Katsumi, T., Benson, C., and Edil, T. (2001). "Hydraulic conductivity and swelling of non-prehydrated GCLs permeated with single species salt solutions." *J. Geotech. Geoenviron. Eng.*, 10.1061/(ASCE)1090-0241(2001)127:7(557), 557–567.
Koerner, R. (2012). *Designing with geosynthetics*, 6th Ed., Vol. 1, Xlibris Corporation, Bloomington, IN.
Kolstad, D., Benson, C., and Edil, T. (2004). "Hydraulic conductivity and swell of nonprehydrated GCLs permeated with multi-species inorganic solutions." *J. Geotech. Geoenviron. Eng.*, 10.1061/(ASCE)1090-0241(2004)130:12(1236), 1236–1249.
LaGatta, M., Boardman, T., Cooley, B., and Daniel, D. (1997). "Geosynthetic clay liners subjected to differential settlement." *J. Geotech. Geoenviron. Eng.*, 10.1061/(ASCE)1090-0241(1997)123:5(402), 402–410.
Meer, S., and Benson, C. (2007). "Hydraulic conductivity of geosynthetic clay liners exhumed from landfill final covers." *J. Geotech. Geoenviron. Eng.*, 10.1061/(ASCE)1090-0241(2007)133:5(550), 550–563.
Mitchell, J., et al. (2007). *Assessment of the performance of engineered waste containment barriers*, National Research Council, National Academies Press, Washington, DC.
Norrish, K., and Quirk, J. (1954). "Crystalline swelling of montmorillonite, use of electrolytes to control swelling." *Nature*, 173(4397), 255–256.
Petrov, R., and Rowe, R. (1997). "Geosynthetic clay liner (GCL)—Chemical compatibility by hydraulic conductivity testing and factors impacting its performance." *Can. Geotech. J.*, 34(6), 863–885.
Rowe, R., and Sangam, H. (2002). "Durability of HDPE geomembranes." *Geotext. Geomembr.*, 20(2), 77–95.
Scalia, J., and Benson, C. (2010a). "Effect of permeant water on the hydraulic conductivity of exhumed GCLs." *Geotech. Test. J.*, 33(3), 201–211.
Scalia, J., and Benson, C. (2010b). "Preferential flow in geosynthetic clay liners exhumed from final covers with composite barriers." *Can. Geotech. J.*, 47(10), 1101–1111.
Scalia, J., and Benson, C. (2011). "Hydraulic conductivity of geosynthetic clay liners exhumed from landfill final covers with composite barriers." *J. Geotech. Geoenviron. Eng.*, 10.1061/(ASCE)GT.1943-5606.0000407, 1–13.
SCDHEC (South Carolina Department of Health and Environmental Control). (2007). "Commercial low-level radioactive waste disposal in South Carolina." *CR-000907*, Bureau of Land and Waste Management, Division of Waste Management, Columbia, SC.
Shackelford, C., Benson, C., Katsumi, T., Edil, T., and Lin, L. (2000). "Evaluating the hydraulic conductivity of GCLs permeated with non-standard liquids." *Geotext. Geomembr.*, 18(2), 133–161.
USEPA (U.S. Environmental Protection Agency). (2007). *Method 6010B: Inductively coupled plasma-atomic emission spectrometry, physical/chemical methods SW846*, 3rd Ed., Office of Solid Waste and Emergency Response, Washington, DC.